Fabrication and Characterization of Self-Assembled β-Cyclodextrin Threaded Monomers and Induced Helical Polymers

Jui-Hsiang Liu,* Yi-Hong Chiu, and Tai-Hsiang Chiu

Department of Chemical Engineering, National Cheng Kung University, Tainan, Taiwan 70101

Received February 23, 2009; Revised Manuscript Received April 8, 2009

ABSTRACT: A novel chiral monomer end-capped with a cholesteryl group and threaded with β-cyclodextrin was synthesized in order to induce the formation of a helical polymer. ^{1}H NMR studies revealed that one or two cyclodextrin molecules were threaded onto the synthesized chiral monomer, leading to the formation of a helical construction of self-assembled inclusion complexes. The formation of a self-assembled inclusion complex was identified using SEM and TEM. The monomeric self-assembled inclusion complex was further polymerized using benzoyl peroxide as a photoinitiator. Both the highly ordered alignment and the helical structure of self-assembled supramolecules were confirmed using polarized optical microscopy and circular dichroism spectroscopy, respectively. We have first demonstrated an easy process for the fabrication of helical polymers via self-assembled monomers threaded with a β-cyclodextrin end and capped with a chiral moiety.

Introduction

Cyclodextrins are naturally produced by the enzymatic conversion of starch. Over the past few years, scientists have found a wide range of applications for these compounds in food, agriculture, environmental engineering, and the pharmaceutical and chemical industries. The ability of cyclodextrins to form complexes with hydrophobic molecules has led to their use in supramolecular chemistry.[1−4] In particular, they have been used to synthesize certain mechanically interlocked molecular architectures, such as rotaxanes and catenanes, by reaction with the ends of a threaded guest.[5,6]

In addition, cyclodextrins are able to form host−guest complexes with hydrophobic molecules based on the unique cyclodextrin structure.[7−12] As a result, cyclodextrins are used for a number of applications in a wide range of fields, including pharmaceutical applications for drug release,[13−15] fluorescence enhancement,[16−18] and solubility enhancement[19] by inclusion complex formation.

The low solubility of β-cyclodextrin, as compared to that of α- and γ-cyclodextrins, is somewhat surprising. This seems to be related to the stronger crystal lattice energy (as with cellulose) resulting from more organized intramolecular hydrogen bonds as well as the similarity to the structure of water resulting in a low entropy of hydration.[20]

Supramolecular chirality has received much interest in recent years.[21−25] In contrast to molecular chirality, in which the atoms of a molecule are arranged in an asymmetric manner in space, supramolecular chirality involves the asymmetric arrangement of molecules by secondary forces.[26−29] We have previously reported the chemistry of a fibrous construction resulting from the self-assembly of inclusion complexes obtained from chiral monomers threaded with β-cyclodextrin.[30] It is known that cholesterol can be used to derive cholesteric liquid crystals with a helical molecule alignment.[31−34] In this paper, in order to emphasize the effect of chirality on the molecular alignment, we report on the synthesis of a novel monomer with a shorter achiral segment and with a cholesteryl group at the terminal end of the monomer. The newly designed chiral monomer was threaded with β-cyclodextrin and formed inclusion complexes. A springlike helical structure of the self-assembled inclusion complex cluster was confirmed using TEM and circular dichroism spectroscopy. We have also demonstrated a novel secondary assembly of a chiral inclusion complex by a chiral monomer threaded with β-cyclodextrin and end-capped with a cholesteryl group.

* Corresponding author. E-mail: jhliu@mail.ncku.edu.tw.

Experimental Section

Materials and Methods. FTIR spectra were recorded on a Jasco VALOR III Fourier transform infrared spectrophotometer. Nuclear magnetic resonance (NMR) spectra were obtained on a Bruker AMX-400 high-resolution NMR spectrometer. Specific rotations were measured at 25 °C in pyridine using a Jasco DIP-360 automatic digital polarimeter with reading precision to 0.001°. Wide-angle X-ray diffraction (WAXD) of the CD and complexes were recorded on a Rigaku D-Max-2200 X-ray powder diffractometer with Cu Kα (1.5406 Å) radiation (40 kV, 40 mÅ). Powder samples were mounted on a sample holder and scanned at a speed of 0.5°/min between $2\theta = 5°$ and 30°. Differential scanning calorimeter (DSC) was conducted with a Perkin-Elmer DSC 7 at a heating and cooling rate of 10 °C min^{-1} in a nitrogen atmosphere. Scanning electron microscope (SEM) microphotographs were measured with a JEOL HR-FESEM JSM-6700F (Osaka, Japan) instrument. The cross-section morphology of the samples was characterized by transmission electron microscopy (TEM) using a JEOL JEM-1200CX-II microscope. The anisotropic properties of the highly ordered self-assembled polymer fibers were investigated by an Olympus BH-2 polarized light microscope (POM) equipped with Mettler hot stage FP-82, and the temperature scanning rate was determined at the rate of 10 °C min^{-1}.

Monomer Preparations. 4-(6-Hydroxyhexyloxy)benzoic acid (HBA) was synthesized as follows. 4-Hydroxybenzoic acid (120 mmol) was dissolved in a mixture of ethanol (42 mL) and water (18 mL), and a solution of potassium hydroxide (318 mmol) and a catalytic amount of potassium iodide dissolved in ethanol (50 mL) were added dropwise. 6-Chloro-1-hexanol (165 mmol) was then added, and the solution was heated at reflux for 24 h. The resulting mixture was poured into water and extracted with ethyl ether. The aqueous solution was acidified with hydrogen chloride diluted with water until it was weakly acidic. The resulting precipitate was filtered and washed several times with water. The crude product was recrystallized from ethanol/water (4/1). Yield: 19.1 g (66.9%), $T_m = 139-140$ °C.

4-(6-Hydroxyhexyloxy)benzoic acid (32 mmol), *N*,*N*-dimethylaniline (33 mmol), and a catalytic amount of 2,6-di-*tert*-butyl-*p*-cresol were dissolved in 1,4-dioxane (50 mL). The solution was cooled in an ice/salt bath, and a solution of acryloyl chloride (100 mmol) in 1,4-dioxane (20 mL) was added dropwise with vigorous stirring. After 24 h at room temperature, the solution was poured

10.1021/ma900406f CCC: $40.75
Published on Web 04/15/2009

Scheme 1

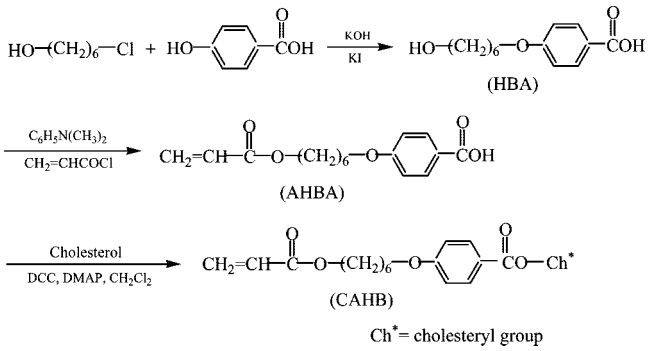

into cold water and the precipitate was filtered. The crude product of 4-(6-acryloyloxyhexyloxy)benzoic acid (AHBA) was washed several times with water and recrystallized twice from ethanol. Yield: 70%; phase transition temperature: crystal 88.0 °C nematic 92.0 °C isotropic. The phase transition temperatures of the product were estimated by differential scanning calorimeter (DSC) and confirmed by polarizing optical microscope (POM).

Cholesteryl-4-(6-acryloyloxyhexyloxy)benzoate (CAHB) was synthesized by reaction of 4-(6-acryloyloxyhexyloxy)benzoic acid (30 mmol) with cholesterol (30 mmol) in the presence of *N*,*N*′-dicyclohexylcarbodiimide (DCC, 87 mmol) and 4-(dimethylamino)pyridine (DMAP, 3 mmol) using dichloromethane (150 mL) as solvent. The reaction mixture was stirred at 30 °C for 24 h. The resulting solution was filtered, washed with water, dried over magnesium sulfate, and evaporated. The crude product was purified by liquid chromatography. Silica gel and ethyl acetate/hexane = 1/8 were used as stationary phase and mobile phase, respectively. The obtained product was recrystallized twice from ethanol. Yield: 56%; phase transition temperature: crystal 101.2 °C nematic 160 °C isotropic; polymerization of the monomer occurred at 160 °C. Scheme 1 shows the synthetic process of the reactions. The synthesized products were identified using ^{1}H NMR and FTIR.

Preparation of Chiral Monomer Threaded with β-Cyclodextrin. To synthesize the inclusion complex, β-cyclodextrin (β-CD) was dissolved in water at 60 °C. CAHB in tetrahydrofuran (THF) was then added, and the resulting reaction mixture was stirred at 60 °C for 24 h. The turbid solution was ultrasonically agitated at room temperature for 15 min, and the clear solution was allowed to stand at room temperature for 2 days. The precipitate was collected, washed thoroughly with THF and then with water to remove the residual CAHB and β-CD, and dried at 60 °C under vacuum.

Polymerization of Self-assembled Monomers. The powdered sample was set on a Petri dish, and benzoyl peroxide (BPO) was used as a photoinitiator. BPO dissolved in methyl ethyl ketone (5 wt %) was dropped onto the powdered inclusion complex. After drying at room temperature, the sample was exposed under UV light for 5 min. The extent of polymerization was monitored using FTIR by following the unsaturated double-bond absorption around 1640 cm^{-1}, which disappeared after UV exposure due to polymerization. The polymerized self-assembled inclusion complex was analyzed using SEM, TEM, and POM. The helical construction of polymerized inclusion complex was analyzed using a JASCO J-715 circular dichroism spectroscopy. For composite film, inclusion complex (30 mmol), methyl mathacrylate (30 mmol), trimethylolpropane triacrylate (10 mmol), and benzoyl peroxide (5 wt %) were dissolved in methyl ethyl ketone. The sample mixture was dropped on a substrate. After drying, the mixture was cured under UV exposure.

Results and Discussion

Synthesis of Monomers Threaded with β-Cyclodextrin. The synthesis of the chiral monomer is shown in Scheme 1. The synthesized compounds were identified using FTIR and NMR. The inclusion complex of β-CD−CAHB was obtained as a white powder with a yield of ∼80%. After thoroughly washing with pyridine and water, the powdered sample no longer contains free monomer or β-cyclodextrin. The purity of the β-CD−CAHB inclusion complexes were confirmed using DSC and FTIR. In the FTIR spectrum, the symmetric and asymmetric −O−H stretching mode of β-CD appeared at 3215−3385 cm^{-1}, and the peaks in the 1700−1800 cm^{-1} region were assigned to the C═O stretching bands of CAHB. The specific rotation of monomer CAHB is −50.2° ($CHCl_3$, 0.01 g/mL). After treatment with β-cyclodextrin, however, the specific rotation of the inclusion complex is +8.08° (pyridine, 0.01 g/mL). This result suggests that the threaded cyclodextrin affects the specific rotation of inclusion complex despite the fact that cyclodextrin is a symmetrical molecule.

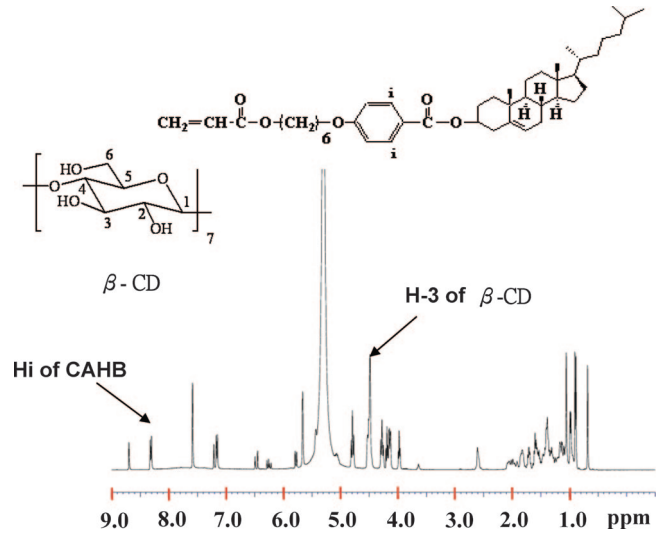

Figure 1. ^{1}H NMR of the β-CD−CAHB inclusion complex. Seven sugar units are present in the β-CD as determined from the peak area ratio. The calculated molar ratio of CD/CAHB is 1.57.

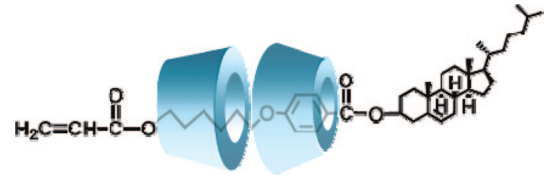

Figure 2. Schematic representation of the cyclodextrin threaded inclusion complex. The calculated value of the CD/CPHB ratio is 1.57. This means that one or two CD molecules were threaded on each CAHB monomer.

The β-CD−CAHB inclusion complex is soluble in pyridine. Its ^{1}H NMR spectrum is shown in Figure 1. The peak area ratio of the characteristic protons of β-CD and CAHB was calculated and found to be 1.57. This result suggests that one or two β-CD molecules were threaded on each monomer. Figure 2 shows a schematic representation of the β-CD threaded CAHB monomer. From the model, the threaded β-CD is expected to improve the molecular interaction between the inclusion complexes. Similarly, the terminal cholesteryl group may offer a chiral effect on the molecular alignment leading to the formation of a helical construction. Theoretically, the chirality effect is quite similar to the induction of a cholesteric phase from nematic liquid crystals by addition of chiral dopants.

Figure 3 shows the DSC curve of the synthesized β-CD−CAHB inclusion complex. In the first heating cycle, absorbed water evaporated around 100 °C.[35] The peak at 195 °C is assigned to the polymerization of the β-cyclodextrin threaded chiral monomers. In the cooling cycle and the second scanning of the sample, no significant peaks were observed. Monomer

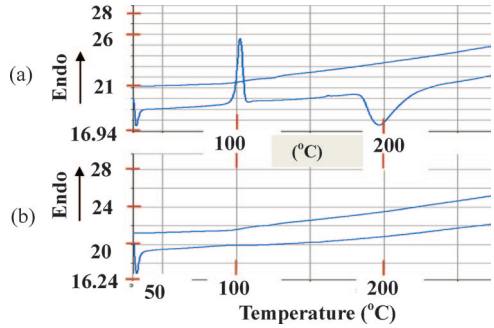

Figure 3. DSC curve of the inclusion complex: (a) water evaporation at 100 °C and polymerization at 195 °C were found in the first heating cycle; (b) no significant peaks were found in the second heating cycle.

CAHB revealed liquid crystalline phases and unthreaded β-cyclodextrin revealed a melting point at about 305 °C. However, no significant peaks could be found at the temperatures of the phase transition points of the monomer by DSC scanning analyses. The results suggest that neither free monomers nor free β-cyclodextrin molecules were in the sample powder. It is noteworthy that the polymerization temperature of the pure monomer is around 160 °C. The polymerization temperature of the inclusion complex of β-cyclodextrin threaded monomer, however, was shifted to 195 °C, as shown in Figure 3. This result suggests an improvement in the thermal resistance of the β-cyclodextrin.

Theoretically, in a polarized optical microscope (POM), the transmitted incident light through the first polarizer is masked by the second perpendicular polarizer. Accordingly, for isotropic materials, no bright image can be seen under POM. As seen in Figure 4a, a significant bright fibrous POM texture corresponding to the self-assembled β-CD−CAHB inclusion complexes was obtained at room temperature. The bright fibrous pattern is ascribed to the highly ordered self-assembled inclusion complex clusters. The birefringent character might be due to the highly ordered self-assembled inclusion complexes. Figure 4b shows an enlarged POM texture of self-assembled β-CD−CAHB inclusion complexes. Polarized light from the bottom polarizer was rotated by the inclusion complex clusters leading to the appearance of the bright pattern. In addition, as shown in Figure 5, fibrous structures with various diameters of the synthesized inclusion complex could be seen by scanning electron microscopy (SEM). The result is consistent with the image obtained by POM.

In order to investigate the construction of self-assembled inclusion complexes, the synthesized sample powder was studied by transmission electron microscopy (TEM). As can be seen in Figure 6a, a springlike helical construction with various diameters was observed. A schematic representation of the sample is shown in Figure 7a. Figure 6b shows the enlargement of the image shown in Figure 6a. An interesting molecular arrangement of the self-assembled inclusion complexes was obtained. To investigate the cross section of the fibrous construction, the columnar constructions were fixed with an epoxy resin, and the sample was sliced with a microtome. Figure 6c shows the cross section of a fixed sample. The outer area is darker, and the central part is lighter. The result is consistent with the image of a top view of a perpendicular spring construction as shown in Figure 7b. Figure 6d shows another cross section of a sliced sample in which the outer spring construction can be seen. This could be due to the columnar construction sloped with a small angle. The sample film is a microtone sliced thin film. Accordingly, only periphery part of the "spring" could be seen. Theoretically, as shown in Figure 7c, the outer spring construction can be seen from a top view

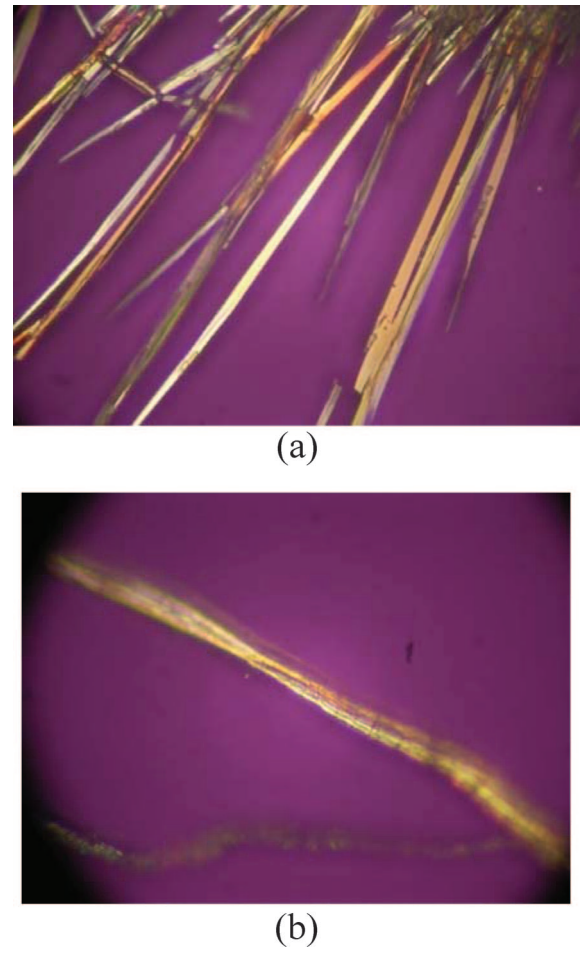

Figure 4. POM textures of the self-assembled inclusion complex. The bright texture represents a highly ordered molecular arrangement of CD−CPHB.

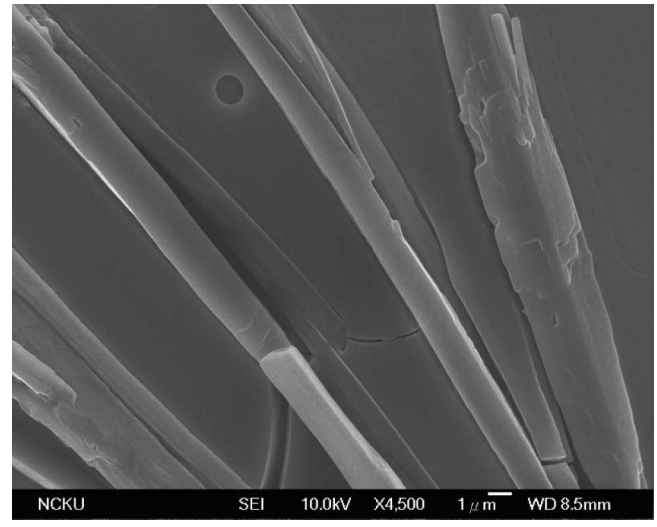

Figure 5. SEM of the β-CD−CPHB inclusion complex. A columnar structure with various diameters was obtained.

of a sloped spring. The TEM images, shown in Figure 6, are completely different from the images obtained in our previous investigation.[29] In our previous paper, the self-assembled inclusion complex revealed only a linear structure. The variation observed in this report could be due to the difference of monomer chirality.

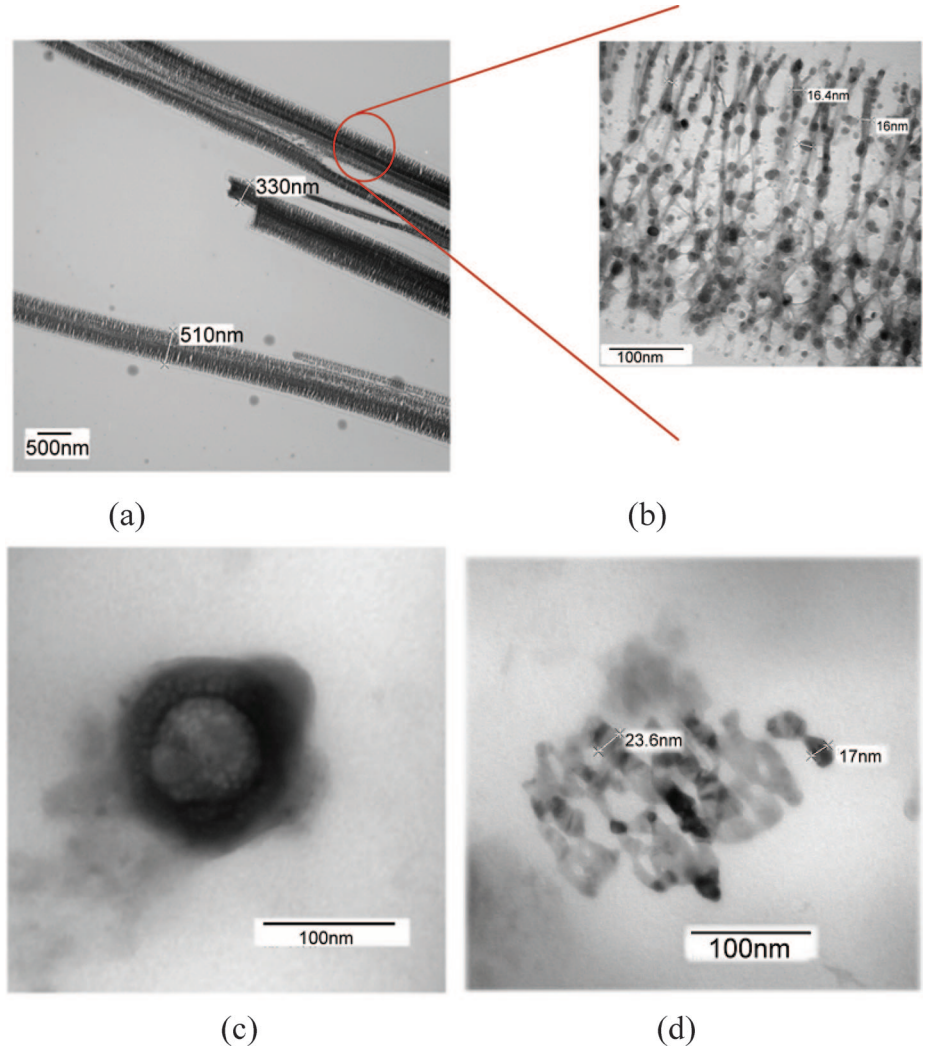

Figure 6. TEM of (a) self-assembled inclusion complex, (b) enlargement of construction in (a), (c) cross section of a helical construction, and (d) cross section of a sloped helical construction.

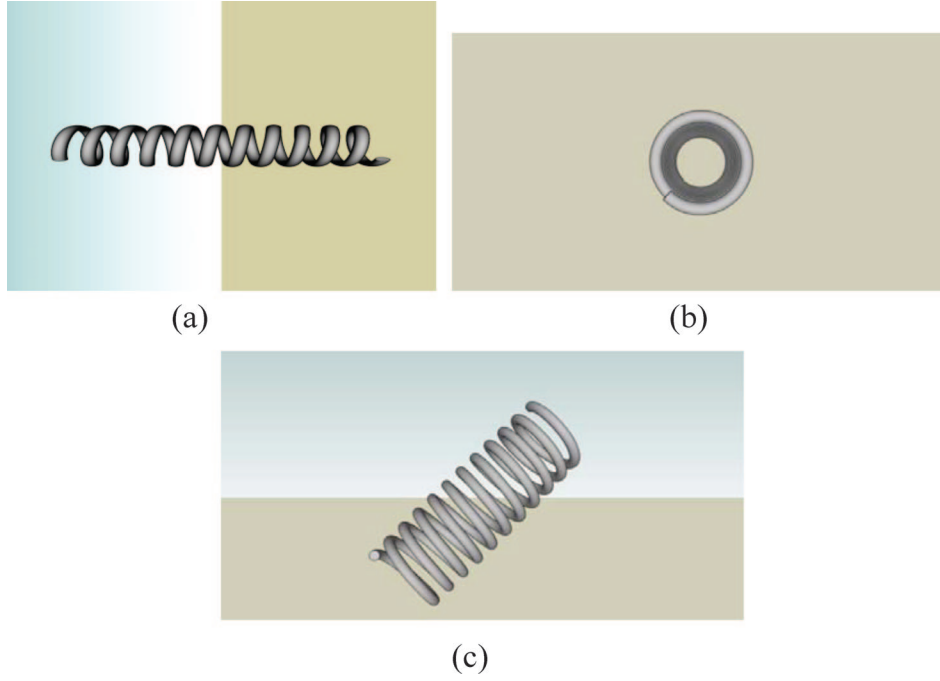

Figure 7. Schematic representation of the samples: (a) a springlike structure, (b) top view of spring, and (c) a sloped spring.

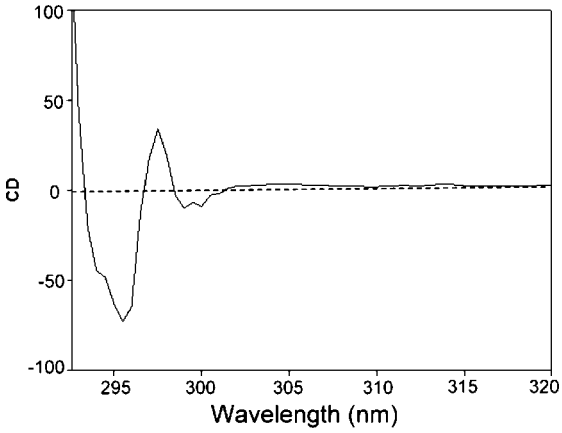

Figure 8. Circular dichroism spectrum of the polymerized self-assembled inclusion complexes.

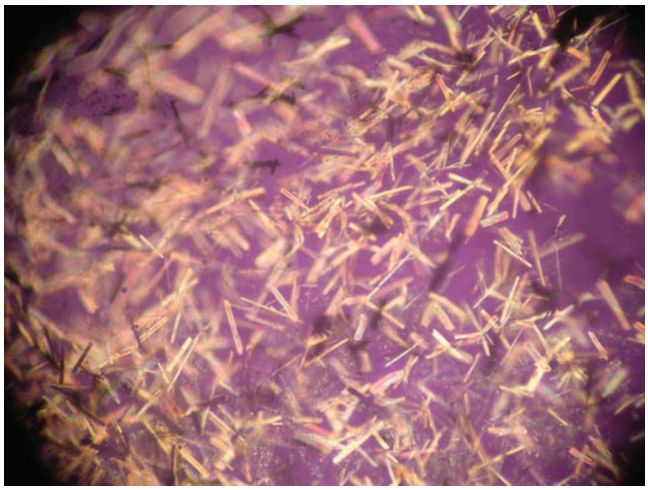

Figure 9. A composite film of MMA, multifunctional acrylate, and synthesized inclusion complex.

Polymerization of β-Cyclodextrin Threaded Monomers. In order to investigate the construction of the self-assembled inclusion complex, the monomeric inclusion complex was polymerized using benzoyl peroxide (BPO). After completion of the UV-initiated polymerization, the polymer was analyzed using POM, SEM, and TEM. The results of POM, SEM, and TEM of the polymerized sample are similar to those of the monomers. The synthesized chiral polymer was further analyzed using circular dichroism (CD) spectroscopy. As shown in Figure 8, a negative Cotton effect could be seen in CD spectrum of the polymer. The result suggests that the synthesized chiral polymer reveals a helical structure.[36] Figure 9 shows an example of a composite film of methyl methacrylate, multifunctional acrylate, and the fibrous inclusion complex synthesized in this investigation. After polymerization, the highly ordered nanofibers are fixed and reveal bright patterns under POM. As seen in Figure 9, nanofibers were fixed in PMMA matrix. The bright fibers mean the highly ordered helical polymer clusters. Because of the existence of the highly ordered polymer fibers, the physical properties of the PMMA matrix are expected to be significantly increased. In this system, cross-linking multifunctional monomers were used. Helical polymers should be cross-linked with PMMA matrix.

As mentioned above, we have demonstrated a simple fabrication of helical polymers via a self-assembly of β-cyclodextrin threaded chiral monomers. This molecular design enabled us to successfully synthesize a chiral inclusion complex and to induce the formation of a helical self-assembled inclusion complex and polymer. Theoretically, as fiber reinforced plastics, the synthesized fibrous monomeric and polymeric self-assembled inclusion complexes are expected to be used in microelectromechanical systems (MEMS) to strengthen the mechanical properties of the nanofilms and the microdevices.

The formation of the inclusion compounds greatly modifies the physical and chemical properties of the guest molecule, mostly in terms of water solubility. The exterior of β-cyclodextrin is sufficiently hydrophilic to impart β-cyclodextrins (or their complexes) water solubility. As seen in Figure 2, the inclusion complex is a chiral compound. Because of the existence of the threaded β-cyclodextrins, molecular interaction between inclusion complexes may be increased, leading to the formation of the supramolecule. Detailed mechanism investigation for the formation of both the self-assembled inclusion complex and the helical construction is now in progress.

Conclusion

A novel chiral monomer end-capped with a cholesteryl group and threaded with β-cyclodextrin was synthesized. One or two CD molecules were found to thread onto the chiral monomer, leading to the formation of a self-assembled helical construction of inclusion complexes. The synthesized self-assembled inclusion complex was polymerized using benzoyl peroxide as a photoinitiator. The helical structure of the monomeric and polymeric inclusion complexes was confirmed using TEM and circular dichroism microscopy. We have developed a novel method for the synthesis of helical polymers via self-assembly of chiral monomers threaded with β-cyclodextrin.

Acknowledgment. The authors thank the National Science Council (NSC) of the Republic of China (Taiwan) for financially supporting this research under Contract 96-2221-E006-009.

Supporting Information Available: FTIR spectra of β-cyclodextrin and β-CD−CAHB inclusion complex, TGA thermogram of self-assembled inclusion complex, heating and cooling DSC thermogram of self-assembled inclusion complex, DSC thermogram of cyclodextrin, circular dichroism spectrum, UV spectrum of polymerized self-assembled inclusion complex, POM textures before and after UV irradiated polymerization, and wide view of the self-assembled inclusion complex. This material is available free of charge via the Internet at http://pubs.acs.org.

References and Notes

(1) Rosenthal, J.; Hodgkiss, J. M.; Young, E. R.; Nocera, D. G. *J. Am. Chem. Soc.* **2006**, *128* (32), 10474.
(2) Liu, Y.; You, C. C.; Zhang, H. Y.; Kang, S. Z.; Zhu, C. F.; Wang, C. *Nano Lett.* **2001**, *1* (11), 613.
(3) Karino, T.; Okumura, Y.; Zhao, C.; Kataoka, T.; Ito, K.; Shibayama, M. *Macromolecules* **2005**, *38* (14), 6161.
(4) Sanji, T.; Kato, N.; Tanaka, M. *Macromolecules* **2006**, *39* (22), 7508.
(5) Alvarez-Pérez, M.; Goldup, S. M.; Leigh, D. A.; Slawin, A. M. Z. *J. Am. Chem. Soc.* **2008**, *130*, 1836.
(6) Brovelli, S.; Latini, G.; Frampton, M. J.; McDonnell, S. O.; Oddy, F. E.; Fenwick, O.; Anderson, H. L.; Cacialli, F. *Nano Lett.* **2008**, *8* (12), 4546.
(7) Brochsztain, S.; Rodrigues, M. A.; Magali, A.; Politi, M. J. *J. Photochem. Photobiol., A* **1997**, *107*, 195.
(8) Amajjahe, S.; Ritter, H. *Macromolecules* **2008**, *41* (3), 716.
(9) Akiyoshi, K.; Ueminami, A.; Kurumada, S.; Nomura, Y. *Macromolecules* **2000**, *33* (18), 6752.
(10) Mascetti, J.; Castano, S.; Cavagnat, D.; Desbat, B. *Langmuir* **2008**, *24* (17), 9616.
(11) Manakker, F.; Pot, M.; Vermonden, T.; Nostrum, C.; Hennink, W. *Macromolecules* **2008**, *41* (5), 1766.
(12) Tsamaloukas, A.; Szadkowska, H.; Slotte, P.; Heerklotz, H. *Biophys. J.* **2005**, *89*, 1109.
(13) Jacobsena, J.; Bjerregaarda, S.; Pedersen, M. *Eur. J. Pharm. Biopharm.* **1999**, *48*, 217.
(14) Loftsson, T.; Matthíasson, K.; Másson, M. *Int. J. Pharm.* **2003**, *262*, 101.

(15) Kazarian, S. G.; Chan, K. L. A. *Macromolecules* **2003**, *36* (26), 9866.
(16) Aghamohammadi, M.; Alizadeh, N. *J. Lumin.* **2007**, *127*, 575.
(17) Raj, C. R.; Ramaraj, R. *J. Photochem. Photobiol., A* **1999**, *122*, 39.
(18) Liu, Y.; Liang, P.; Chen, Y.; Zhang, Y. M.; Zheng, J. Y.; Yue, H. *Macromolecules* **2005**, *38* (22), 9095.
(19) Rawata, S.; Jain, S. K. *Eur. J. Pharm. Biopharm.* **2004**, *57*, 263.
(20) Jursic, B. S.; Zdravkovski, Z.; French, A. D. *J. Mol. Struct.* **1996**, *366*, 113.
(21) Johnson, R. S.; Yamazaki, T.; Kovalenko, A.; Fenniri, H. *J. Am. Chem. Soc.* **2007**, *129* (17), 5735.
(22) Harada, A. *Supramol. Sci.* **1996**, *3*, 19.
(23) Caskey, D. C.; Yamamoto, T.; Addicott, C.; Shoemaker, R. K.; Vacek, J.; Hawkridge, A. M.; Muddiman, D. C.; Kottas, G. S.; Michl, J.; Stang, P. J. *J. Am. Chem. Soc.* **2008**, *130* (24), 7620.
(24) Kim, S. A.; Jung, D. H.; Kim, Y. H.; Kang, M. A.; Jung, H. T. *Macromolecules* **2006**, *39* (18), 6186.
(25) Xiao, S.; Lu, X.; Lu, Q.; Su, B. *Macromolecules* **2008**, *41* (11), 3884.
(26) Rai, R.; Saxena, A.; Ohira, A.; Fujiki, M. *Langmuir* **2005**, *21* (9), 3957.
(27) Zhang, L.; Li, X.; Mu, J. *Colloids Surf., A* **2007**, *302*, 219.
(28) Zhu, H.; Dong, H.; Huang, W.; Gou, S. *J. Mol. Struct.* **2007**, *831*, 55.
(29) Wu, A.; Shen, X.; He, Y. *J. Colloid Interface Sci.* **2006**, *302*, 87.
(30) Liu, J. H.; Harada, A.; Hung, H. J. *Langmuir* **2008**, *24*, 7442.
(31) Nagai, K.; Sakajiri, K.; Maeda, K.; Okoshi, K.; Sato, T.; Yashima, E. *Macromolecules* **2006**, *39* (16), 5371.
(32) Goto, H. *Macromolecules* **2007**, *40* (5), 1377.
(33) Smalyukh, B. I.; Lavrentovich, O. D. *Opt. Lett.* **2005**, *30* (4), 349.
(34) Hwang, J.; Ha, N. Y.; Chang, H. J.; Park, B.; Wu, J. W. *Opt. Lett.* **2004**, *29* (22), 2644.
(35) Hedges, A. R. *Chem. Rev.* **1998**, *98* (5), 2035.
(36) Okoshi, K.; Nagai, K.; Kajitani, T.; Sakurai, S.; Yashima, E. *Macromolecules* **2008**, *41* (20), 7752.

MA900406F